Desalination and Water Treatment
www.deswater.com

doi: 10.5004/dwt.2022.286456

266 (2022) 154–162
August

Preparation of Zn^{2+}-Ni^{2+}-Fe^{3+}-LDHs and study on photocatalytic degradation of phenol

Xiaoli Song, Yuxiu Fu, Yaming Pang, Liguo Gao*, Xiangrong Ma

School of Chemistry and Chemical Engineering, Yulin University, Yulin 719000, Shannxi, China,
Tel. +86 09123891144; emails: liguogao2008@163.com/liguogao@yulinu.edu.cn (L. Gao), songxiaoli2004@163.com (X. Song), 1971545865@qq.com (Y. Fu), 986827945@qq.com (Y. Pang), maxiangrong615@163.com (X. Ma)

Received 6 February 2022; Accepted 10 June 2022

ABSTRACT

Using urea as complexing agent, Zn^{2+}-Ni^{2+}-Fe^{3+}-LDHs were successfully prepared by homogeneous precipitation method (molar ratio 1:6:2). UV diffuse reflectance spectroscopy results show that the Zn^{2+}-Ni^{2+}-Fe^{3+}-LDHs have a narrower band gap (2.00 eV) and higher catalytic activity. This work utilizes Zn^{2+}-Ni^{2+}-Fe^{3+}-LDHs for photocatalytic degradation of phenol. The conditions for degrading phenol were optimized by response surface methodology, and the reaction mechanism of layered double hydroxides (LDHs) photocatalytic degradation of phenol was obtained. The results showed that when the concentration of phenol was 12 mg L^{-1}, the dosage of Zn^{2+}-Ni^{2+}-Fe^{3+}-LDHs was 0.020 g, the dosage of NaS_2O_8 was 0.022 g, and the visible light irradiation time was 86 min, the phenol clearance rate reached 91.18%.

Keywords: Layered double hydroxides; Phenol; Adsorption; Photocatalytic degradation

1. Introduction

The phenolic organic pollutants in industrial wastewater have complex molecular structures, stable properties and high toxicity, which are difficult to treat by traditional methods [1–4]. Photocatalytic technology provides an effective method to solve the problem of industrial wastewater treatment, and has become one of the hot spots in the field of wastewater treatment research [5]. Layered double hydroxides (LDHs) compounds are layered compounds composed of positively charged metal hydroxide layers and interlayer anions. The general formula is $[M^{2+}_{1-x}\ M^{3+}_{x}(OH)_2]^{x+}(A^{n-})_{x/n}\cdot mH_2O$, where M^{2+} and M^{3+} can convert divalent and trivalent metal cations on the laminate, and A^{n-} is the layer inter anion. In general, LDHs materials containing transition metal cations (Zn^{2+}, Cu^{2+}, Mg^{2+}) in the hydroxide layer are valuable as photocatalysts with electron transfer ability and excellent geometric characteristics [6]. However, Zn-LDHs have been widely used in the photocatalytic degradation of water due to their high photocatalytic activity, chemical stability, and low toxicity. Zn-LDHs have suitable band structures (band gap, valence band edge, conduction band edge) [7–10]. Zn-LDHs can be used as photocatalysts to remove various organic pollutants, which is beneficial to the advanced oxidation of •OH. Nickel-containing compounds are widely used semiconductor materials. If Ni(II) and a certain trivalent metal ion can be constructed into a hydrotalcite-like structure and Ni(II) can be co-catalyzed, better catalytic performance is expected. Generally, Al^{3+} is selected as the trivalent metal ion of LDHs, mainly because Al^{3+} has amphoteric properties and is close to the precipitation pH value of divalent metal ions, which is conducive to the formation of LDHs layered structure [11]. However, Song et al. [12] demonstrated the lower band gap and higher photocatalytic efficiency of Ni-Fe-LDHs than Ni-Al-LDHs using density of states first-principles. Han et al. [13] demonstrated that the formation of magnetic Fe^{3+}-LDHs nanoparticles can be easily separated with the help of an

* Corresponding author.

external magnetic field, which makes the catalyst easy to recycle. Therefore, a novel Zn^{2+}-Ni^{2+}-Fe^{3+}-LDHs photocatalyst was prepared for the first time. The response surface methodology was used to optimize the conditions of phenol degradation, and then the reaction mechanism of LDHs photocatalytic degradation of phenol was obtained [14–16].

2. Experimental

2.1. Materials

Zinc nitrate ($Zn(NO_3)_2$ $6H_2O$); nickel nitrate ($Ni(NO_3)_3$ $6H_2O$); ferric chloride ($Fe(Cl)_3$ $6H_2O$); urea ($CO(NH_2)_2$); phenol (C_6H_5OH); absolute ethanol (CH_3CH_2OH); potassium ferricyanide ($K_3[Fe(CN)_6]$); sodium persulfate ($Na_2S_2O_8$); ammonia water (NH_4OH); ammonium chloride (NH_4Cl); 4-aminoantipyrine ($C_{11}H_{13}N_3O$). The above reagents are all Analytical grade, potassium bromide (KBr) barium sulfate ($BaSO_4$) is spectrally pure.

2.2. Preparation of Zn^{2+}-Ni^{2+}-Fe^{3+}-LDHs

In the standard experiment, the molar ratio of Zn^{2+}, Ni^{2+}, Fe^{3+} is 1:6:2. Accurately weight 0.5948 g ($Zn(NO_3)_2{\cdot}6H_2O$), 4.3620 g ($Ni(NO_3)_3{\cdot}9H_2O$), 1.3514 g ($Fe(Cl)_3{\cdot}4H_2O$) and 3.3784 g ($CO(NH_2)_2$) with an analytical balance and dissolve them in 100 mL of ultrapure water. The prepared solution was sonicated in an ultrasonic apparatus for 5 min. After the solution was uniform, the solution was immediately transferred to a high-pressure reactor, and the temperature was set to 150°C in the homogeneous reactor for 48 h of continuous reaction. Finally, the solution was suction filtered. During the suction filtration process, first wash with ultrapure water 2–3 times, and then wash with absolute ethanol 2–3 times. The samples were naturally dried at room temperature and then ground into powder to obtain Zn^{2+}-Ni^{2+}-Fe^{3+}-LDHs samples.

2.3. Testing and characterization

Measure 1, 2, 4, 6, and 8 mL of 50 mg L^{-1} phenol solution and put them into 50 mL colorimetric tubes respectively. The color was developed by 4-aminoantipyrine method, and then the absorbance of phenol at different concentrations were measured by UV-Vis analytical spectrometer. The standard curve for phenol is shown in Fig. 1.

Measure 20 mL of 12 mg L^{-1} phenol solution with a pipette into a colorimetric tube, add a certain amount of Zn^{2+}-Ni^{2+}-Fe^{3+}-LDHs to it, control a certain temperature and time, and then filter. The absorbance of the filtrate was measured at a wavelength of 510 nm in a UV-Vis spectrophotometer and the absorbance of distilled water was used as a reference. The calculation method of phenol removal rate is as follows:

$$R = \frac{A_0 - A_i}{A_0} \times 100\% \quad (1)$$

where A_0 represents the absorbance of the phenol solution before treatment, A_i represents the absorbance of the phenol solution after treatment, and R represents the removal rate of phenol (%).

3. Results and discussion

3.1. Analysis with scanning electron microscopy

Fig. 2 is the scanning electron microscopy (SEM) image of the Zn^{2+}-Ni^{2+}-Fe^{3+}-LDHs sample. It can be seen from the graphs of different scales that the prepared exhibit a uniform layered structure [17]. It is further confirmed that the prepared product conforms to the special structure of hydrotalcite-like compounds.

3.2. Analysis with EDS

Fig. 3 and Table 1 show that zinc, nickel and iron are present in the samples. It shows that Zn^{2+}-Ni^{2+}-Fe^{3+}-LDHs was successfully prepared.

3.3. Analysis with Fourier transform infrared spectroscopy

In Fig. S1, 3,438 cm^{-1} represents the stretching vibration of the O–H bond between the plates and the O–H bond in the water molecule. The characteristic peak around 1,378 cm^{-1} is the asymmetric stretching vibration peak of O–C–O, which can prove the existence of CO_3^{2-} between the hydrotalcite layers [18]. It shows that the intercalation of carbonate is successful. At 674 cm^{-1}, it is the characteristic peak of vibration correlation between metal and oxygen, which belongs to the landmark peak of LDHs.

3.4. Study on BET specific surface area and pore-size distribution

Fig. 4 shows the nitrogen adsorption and desorption isotherms of Zn^{2+}-Ni^{2+}-Fe^{3+}-LDHs samples have small plateaus and hysteresis loops, indicating that the obtained products have the characteristics of mesoporous materials [19]. The BET specific surface area is 137.187 m^2 g^{-1}, indicating that the product has many interlayer pores and large pore size, so it has a good adsorption effect on phenol.

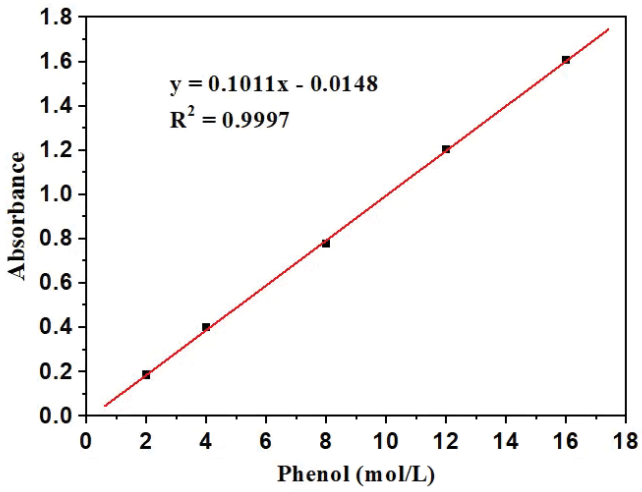

Fig. 1. Standard curve for phenol.

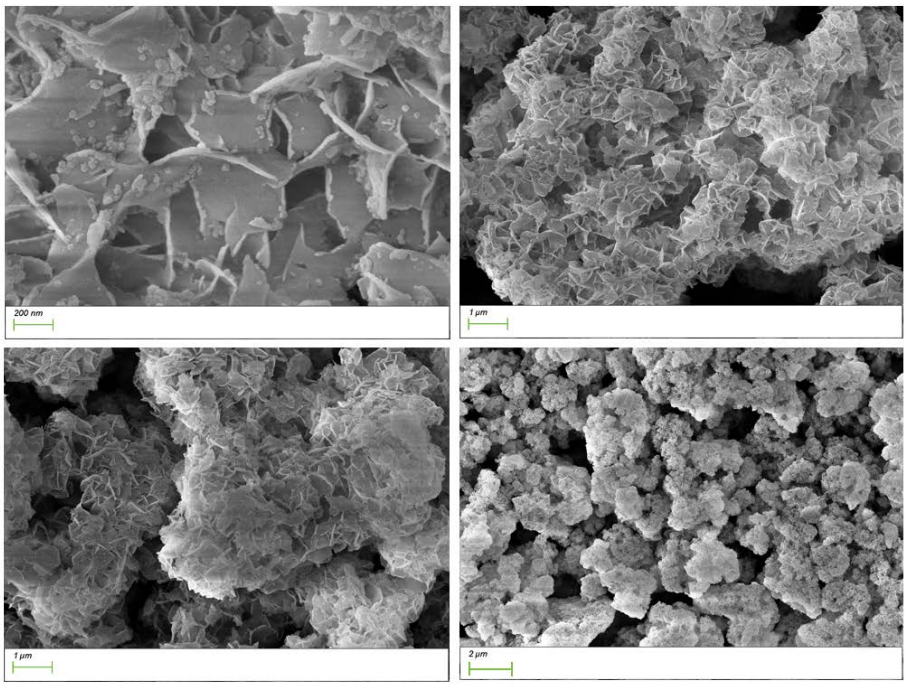

Fig. 2. SEM micrographs of samples.

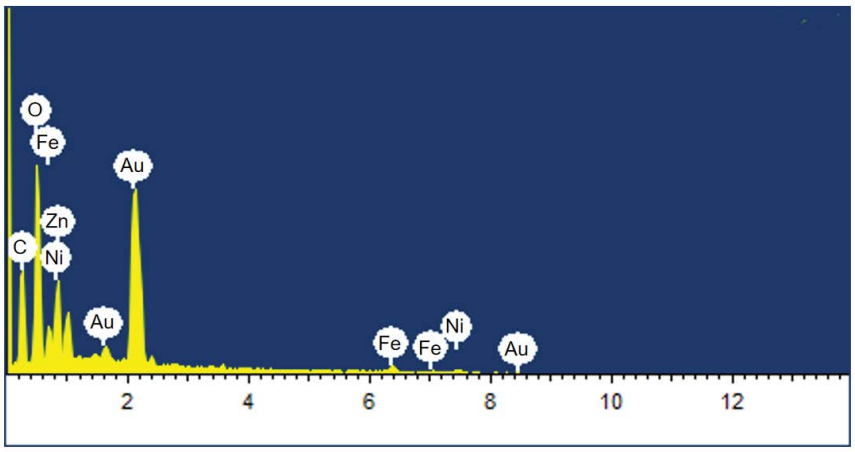

Fig. 3. Elemental analysis diagrams of samples.

Fig. 5 shows the pore-size distribution of the Zn^{2+}-Ni^{2+}-Fe^{3+}-LDHs sample. It can be seen from the figure that the sample has a certain distribution at 40–170 nm, and a higher peak appears at 80 nm, indicating that most of the pore diameters in the sample are 80 nm.

3.5. Analysis with UV

UV diffuse reflectance spectroscopy can further verify the photocatalytic performance of the material. It can be seen from Fig. 6 that the absorption wavelength of Zn^{2+}-Ni^{2+}-Fe^{3+}-LDHs is 619 nm. According to $E_g = hc/\lambda$ (E_g = 1,240/λ). It can be seen that the forbidden band widths of Zn^{2+}-Ni^{2+}-Fe^{3+}-LDHs are 2.00 eV. According to the solid band theory and photocatalytic mechanism, the smaller the forbidden band width, the easier the valence electrons on the catalyst are excited, resulting in the generation of photo-generated holes and photo-generated electrons with high activity, and the higher the catalytic activity [20].

3.6. Response surface analysis

The degradation conditions of phenol by Zn^{2+}-Ni^{2+}-Fe^{3+}-LDHs were optimized by single factor experiment. The effects of catalyst dosage, oxidant dosage, time and light condition on the photocatalytic degradation of phenol were studied. (1) Measure 20 mL of 12 mg L^{-1} phenol standard solution and place them in 6 colorimetric tubes,

Table 1
Spectral analysis of samples and their element content

Element	Zn^{2+}	Ni^{2+}	Fe^{3+}
Line type	L	L	L
Weight percentage	2.71	19.03	5.29
Atomic percentage	1.56	10.78	3.58

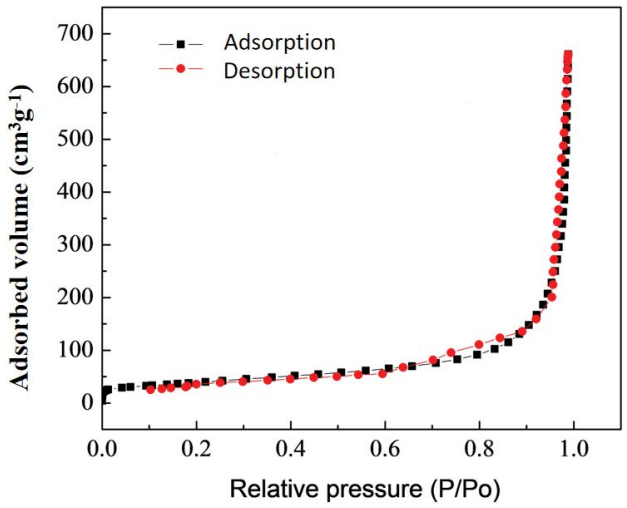

Fig. 4. The adsorption and desorption isotherms of the samples.

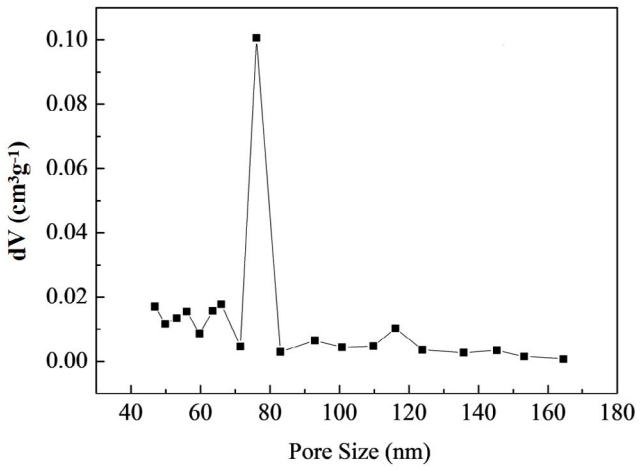

Fig. 5. Pore-size distribution of the samples.

add 0.025 g of NaS_2O_8, and respectively add 0.005, 0.010, 0.015, 0.020, 0.025 and 0.030 g of Zn^{2+}-Ni^{2+}-Fe^{3+}-LDHs were adsorbed under dark light for 30 min at room temperature and degraded under visible light for 100 min. (2) Measure 20 mL of 12 mg L^{-1} phenol standard solution and place them in 5 colorimetric tubes, add 0.025 g of Zn^{2+}-Ni^{2+}-Fe^{3+}-LDHs, and respectively add 0.010, 0.015, 0.020, 0.025 and 0.030 g of NaS_2O_8 were adsorbed under dark light for 30 min at room temperature and degraded under visible light for 100 min.

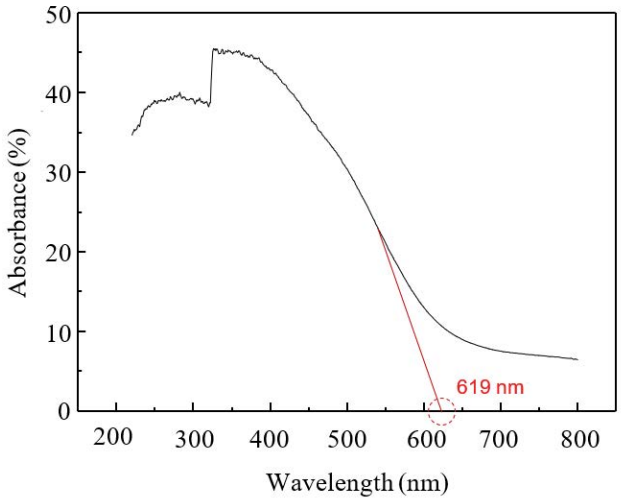

Fig. 6. UV diffuse reflectance spectra of samples.

(3) Measure 20 mL of 12 mg L^{-1} phenol solution into a colorimetric tube, add 0.025 g of Zn^{2+}-Ni^{2+}-Fe^{3+}-LDHs and 0.025 g NaS_2O_8 respectively, adsorb under dark light for 30 min, then degrade under visible light, every interval 20 min sampling. (4) Measure 20 mL of 12 mg L^{-1} phenol solution and add it to 3 colorimetric tubes, and then add the same amount of 0.025 g of Zn^{2+}-Ni^{2+}-Fe^{3+}-LDHs and NaS_2O_8. They were placed under ultraviolet light, visible light, and dark light and stirred for 100 min. Calculate the clearance rate of phenol according to Eq. (1). Fig. 7 shows that the clearance rate increases with the increase of the added amount of catalyst when the amount of catalyst added is small, and the degradation effect is the best when the amount of catalyst is 0.025 g. However, when the amount of catalyst added is too high, the degradation rate decreases. When the dosage of NaS_2O_8 was 0.010–0.025 g, the photodegradation rate of phenol increased with the increase of the dosage of NaS_2O_8. Because the dosage of the oxidant NaS_2O_8 increases, more free radicals will be generated in the system, and the free radicals will react with them to make the phenol degraded better [21]. If the dosage of NaS_2O_8 is greater than 0.025 g, excess free radicals will be generated, resulting in the reaction between free radicals, and the degradation rate of phenol will decrease. The clearance rate of phenol also increased with the prolongation of illumination time. When the time increased to 100 min, the degradation rate of phenol decreased, because the adsorption and photocatalytic oxidation effects existed in a short time, which made LDHs achieve a higher degradation effect in a short time. The scavenging rates under UV light and visible light are similar, and in terms of economic benefits, it is more suitable to degrade phenol under visible light. Therefore, Zn^{2+}-Ni^{2+}-Fe^{3+}-LDHs is 0.025 g, NaS_2O_8 is 0.025 g, and the clearance rate of phenol is relatively high under visible light irradiation for 100 min.

Table 2 shows the Box–Behnken experimental design and results display. Table 3 shows the significance test of the regression equation coefficients. It can be seen from the table that when $P < 0.0100$, the indicator is extremely significant;

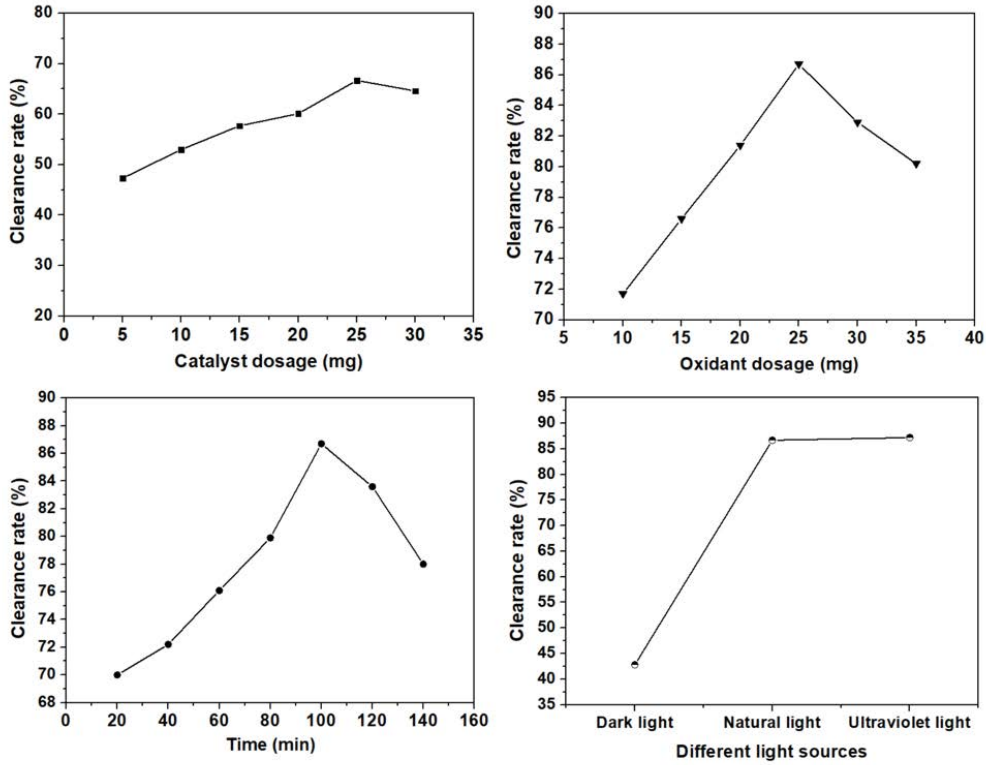

Fig. 7. Single factor experiments under different conditions.

Table 2
Box–Behnken experimental design and results display

No.	Catalyst dosage (g)	Oxidant dosage (g)	Time (min)	Clearance rate (%)
1	0.025	0.010	40	70.3
2	0.025	0.025	100	86.7
3	0.015	0.010	100	78.0
4	0.015	0.025	120	78.8
5	0.025	0.025	100	86.7
6	0.015	0.035	100	80.2
7	0.030	0.025	40	72.4
8	0.025	0.025	100	86.7
9	0.025	0.035	40	72.1
10	0.030	0.025	120	83.2
11	0.015	0.025	40	71.6
12	0.030	0.035	100	81.6
13	0.025	0.025	100	86.7
14	0.025	0.010	120	80.1
15	0.025	0.025	100	86.7
16	0.030	0.010	100	79.3
17	0.025	0.035	120	82.6

Table 3
Significance test of regression equation coefficient

	Sum of square	Degree of freedom	Mean square	*F*	*P*
Model	531.72	9	59.08	181.23	<0.0001
A-Catalyst dosage	4.49	1	4.49	13.76	0.0076
B-Oxidant dosage	7.44	1	7.44	22.82	0.0020
C-Time	162.39	1	162.39	498.16	<0.0001
AB	0.060	1	0.060	0.18	0.0418
AC	2.44	1	2.44	7.49	0.0290
BC	0.093	1	0.093	0.29	0.0095
A^2	36.05	1	36.05	110.59	<0.0001
B^2	44.50	1	44.50	136.51	<0.0001
C^2	73.69	1	73.69	226.05	<0.0001
Residual	2.28	7	0.33		
Sum	534.00	16			
R^2	0.9957				

when $P < 0.0500$, the indicator is significant; when $P > 0.0500$, the indicator is insignificant. The quadratic equation model $P < 0.0100$ indicates that the model is extremely significant, so it is the real point that the regression equation can be used to simulate the equation test. The correlation coefficient of the regression model is $R^2 = 0.9957$, which indicates that 99.57% of the corresponding data points can be explained by the linear relationship of this equation. It can be seen from the table that the *P*-values of *A*, *B*, *C*, A^2, B^2, C^2, *AB*, *AC*, *BC* are less than 0.0500, indicating a significant

factor. The *P*-value of the interaction item < 0.0500 was considered significant, while the *P*-values of *AC*, *BC* and *AB* of the interaction item were all less than 0.05, which was considered significant or extremely significant. From the value of F, it can be compared that the order of factors affecting the scavenging effect of Zn^{2+}-Ni^{2+}-Fe^{3+}-LDHs on phenol is: light time > dosage of sodium persulfate > dosage of hydrotalcites.

Fig. 8 shows the contour and three-dimensional response surface plots of the interaction term to explore the effect of the interaction term on the phenol clearance rate by taking the *AB* interaction term as an example. The curved surface figure is convex, which can indicate that there is a maximum value within the test range of the experimental model [22]. It can be seen from the figure that with the increase of the amount of *A* (catalyst) and *B* (oxidant), the scavenging rate gradually increases. When the catalyst reaches 0.020 g and the oxidant reaches 0.022 g, the scavenging rate of phenol reaches the maximum. Interaction to get a suitable reaction time. Through the optimization and analysis of the experimental model, the optimal conditions were obtained: when the catalyst dosage was 0.020 g, the oxidant dosage was 0.022 g, and the time was 86 min, the phenol removal rate could reach 91.18%.

3.7. Photocatalytic reaction pollution assessment

In order to verify that the degradation of phenol by Zn^{2+}-Ni^{2+}-Fe^{3+}-LDHs will not cause secondary pollution, the wastewater solution before and after degradation was measured by Fourier transform infrared spectroscopy (FTIR). It can be seen from Fig. S2 that the solution before degradation has a hydroxyl absorption peak near 3,235 cm^{-1}, and a benzene ring absorption peak at 1,600~1,500 cm^{-1} [23–26]. In the solution after degradation, the absorption peaks of hydroxyl and benzene ring disappeared, and the stretching vibration peak of CO_3^{2-} appeared in the range of 1,300~872 cm^{-1}. This shows that Zn^{2+}-Ni^{2+}-Fe^{3+}-LDHs completely catalyzes the oxidation of phenol to CO_2 and H_2O without causing secondary pollution.

3.8. Prediction of photocatalytic reaction mechanism

Fig. 9 shows the catalytic oxidation process of phenol by Zn^{2+}-Ni^{2+}-Fe^{3+}-LDHs catalyst. Through the experimental results and previous research work, we predicted a mechanism. First, when the Zn^{2+}-Ni^{2+}-Fe^{3+}-LDHs molecule absorbs the energy of light, an electron hole (h^+) and photogenerated electron (e^-) are generated. At the same time, SO_4^- produced by sodium persulfate reacts with water to form •OH [27–32]. Therefore, phenol can be efficiently catalytically oxidized to carbon dioxide and water.

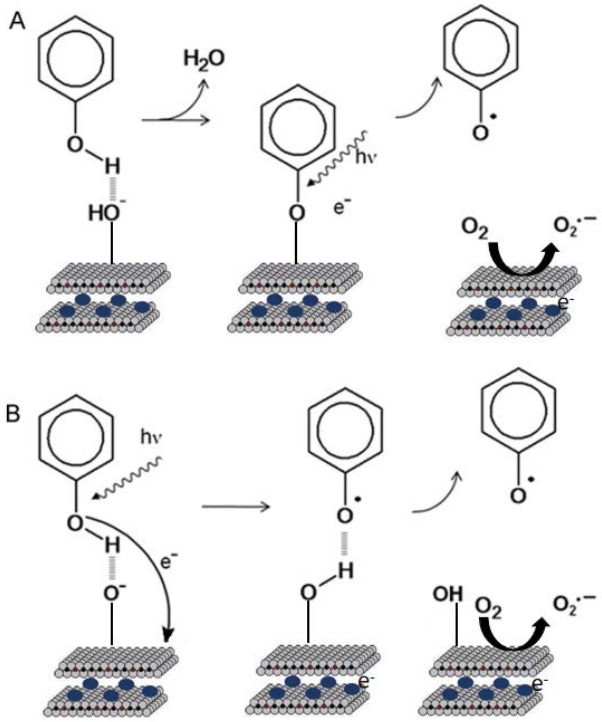

Fig. 9. Catalytic oxidation process of phenol on Zn^{2+}-Ni^{2+}-Fe^{3+}-LDHs.

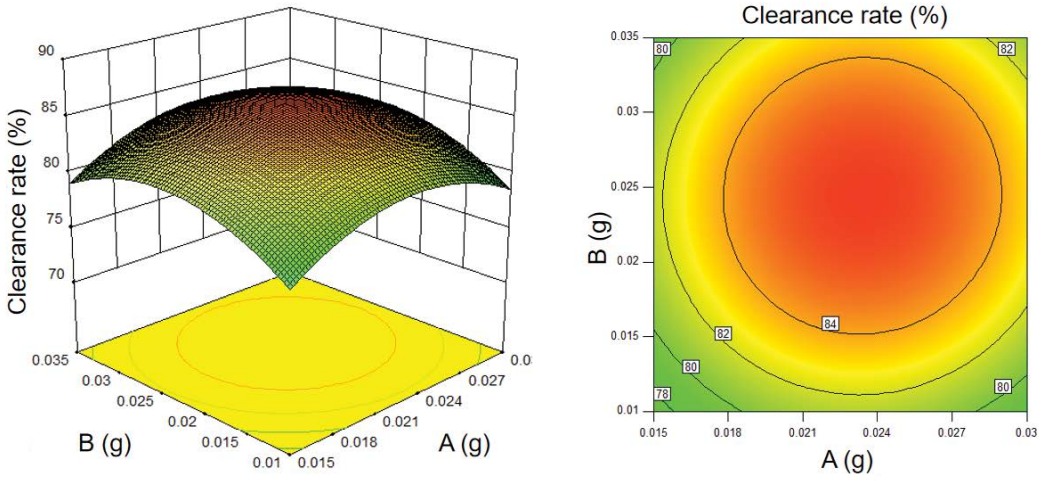

Fig. 8. Contour and surface plots of interaction terms affecting clearance rate.

$$Zn^{2+} - Ni^{2+} - Fe^{3+} - LDHs + hv \rightarrow \left(e^{-}\right) + \left(h^{+}\right) \quad (1)$$

$$\left(h^{+}\right) + H_2O \rightarrow OH^{\bullet} + H^{+} \quad (2)$$

$$S_2O_8^{2-} + SO_4^{-\bullet} \rightarrow SO_4^{2-} + OH^{\bullet} + H^{+} \quad (3)$$

$$H_2O + SO_4^{-\bullet} \rightarrow SO_4^{2-} + {}^{\bullet}OH + H^{+} \quad (4)$$

$$\begin{aligned} {}^{\bullet}OH + C_6H_5OH &\rightarrow C_6H_6O_2 \\ &\rightarrow HOOC - CH = CH - COOH \\ &\rightarrow CO_2 + H_2O \end{aligned} \quad (5)$$

3.9. Determination of hydroxyl radicals

Fig. S3 is to verify the presence of •OH. Ce^{3+} can produce characteristic fluorescence in dilute sulfuric acid medium, and its maximum excitation wavelength and emission wavelength are 280 and 360 nm, respectively [33]. When Ce^{3+} is oxidized by •OH to non-fluorescent Ce^{4+}, the characteristic fluorescence disappears and the fluorescence peak at 360 nm changes. This indicates that •OH was produced during the reaction. Its measurement principle can be expressed as: $Ce^{3+} + {}^{\bullet}OH = H^{+}Ce^{4+} + H_2O$.

4. Conclusion

Zn^{2+}-Ni^{2+}-Fe^{3+}-LDHs were synthesized by a simple, economical and environment friendly method. The crystal structure, elemental composition and material properties of the samples were characterized by Fourier transform infrared spectroscopy, SEM, energy dispersive analysis, UV-visible photometer and X-ray diffraction. Clearance rate of phenol was obtained by the 4-aminoantipyrine method. The results show: (1) Zn^{2+}-Ni^{2+}-Fe^{3+}-LDHs have larger specific surface area and pore size, so this sample has higher adsorption performance for phenol. (2) The characterization of UV diffuse reflection and the prediction of the photocatalytic mechanism show that the forbidden band width of Zn^{2+}-Ni^{2+}-Fe^{3+}-LDHs is smaller, and when hv energy enters, it will generate highly active hole-electron pairs. After the reaction a large amount of •OH is produced, which can oxidize phenol to carbon dioxide and water. (3) The magnetic properties of Zn^{2+}-Ni^{2+}-Fe^{3+}-LDHs facilitate recycling. (4) The conditions for the best performance of LDHs were obtained by changing different factors and conducting response surface optimization experiments. The results showed that when the concentration of phenol was 12 mg L^{-1}, the dosage of Zn^{2+}-Ni^{2+}-Fe^{3+}-LDHs was 0.020 g, the dosage of NaS_2O_8 was 0.022 g and the visible light irradiation time was 86 min, the removal rate of phenol reached 91.18%.

Acknowledgements

This work was subsidized by the Science and Technology Department of Shaanxi Province (2020QFY05-05), Joint Foundation of University of Chinese Academy of Sciences and Yulin University (2021003 and 2021019) and Yulin High-tech Zone Science and Technology Bureau (CXY-2020-031 and CXY-2021-22).

References

[1] L. Zhang, C.-h. Dai, X.-x. Zhang, Y.-n. Liu, J.-h. Yan, Synthesis and highly efficient photocatalytic activity of mixed oxides derived from ZnNiAl layered double hydroxides, Trans. Nonferrous Met. Soc. China, 26 (2016) 2380–2389.
[2] L. Yang, D. Xu, H. Yang, X. Luo, H. Liang, Structurally-controlled FeNi LDH/CNTs electro-Fenton membrane for in-situ electro-generation and activation of hydroxyl radicals toward organic micropollutant treatment, Chem. Eng. J., 432 (2022) 134436, doi: 10.1016/j.cej.2021.134436.
[3] G. Morales-Mendoza, M. Alvarez-Lemus, R. López, F. Tzompantzi, R. Adhikari, S.W. Lee, L.M. Torres-Martínez, R. Gómez, Combination of Mn oxidation states improves the photocatalytic degradation of phenol with ZnAl LDH materials without a source of O_2 in the reaction system, Catal. Today, 266 (2016) 62–71.
[4] J. Wang, J. Tang, Fe-based Fenton-like catalysts for water treatment: catalytic mechanisms and applications, J. Mol. Liq., 332 (2021) 115755, doi: 10.1016/j.molliq.2021.115755.
[5] H. Wang, Z. Zhang, M. Jing, S. Tang, Y. Wu, W. Liu, Synthesis of CuNiSn LDHs as highly efficient Fenton catalysts for degradation of phenol, Appl. Clay Sci., 186 (2020) 105433, doi: 10.1016/j.clay.2019.105433.
[6] H. Wang, M. Jing, Y. Wu, W. Chen, Y. Ran, Effective degradation of phenol via Fenton reaction over CuNiFe layered double hydroxides, J. Hazard. Mater., 353 (2018) 53–61.
[7] F. Tzompantzi, A. Mantilla, F. Bañuelos, J.L. Fernández, R. Gómez, Improved photocatalytic degradation of phenolic compounds with ZnAl mixed oxides obtained from LDH materials, Top. Catal., 54 (2011) 257–263.
[8] A. Tripathi, C.M. Hussain, ZnAl-LDH and B-impregnated polymeric semiconductor (g-C_3N_4) for solar light-driven photocatalysis to treat phenolic effluent, Sustainable Mater. Technol., 28 (2021) e00266, doi: 10.1016/j.susmat.2021.e00266.
[9] Á. Patzkó, R. Kun, V. Hornok, I. Dékány, T. Engelhardt, N. Schall, ZnAl-layer double hydroxides as photocatalysts for oxidation of phenol in aqueous solution, Colloids Surf., A, 265 (2005) 64–72.
[10] P.Y. Motlagh, A. Khataee, A. Hassani, T. Sadeghi Rad, ZnFe-LDH/GO nanocomposite coated on the glass support as a highly efficient catalyst for visible light photodegradation of an emerging pollutant, J. Mol. Liq., 302 (2020) 112532, doi: 10.1016/j.molliq.2020.112532.
[11] L. Wang, Z. Zhu, F. Wang, Y. Qi, W. Zhang, C. Wang, State-of-the-art and prospects of Zn-containing layered double hydroxides (Zn-LDH)-based materials for photocatalytic water remediation, Chemosphere, 278 (2021) 130367, doi: 10.1016/j.chemosphere.2021.130367.
[12] X. Song, Y. Pang, Y. Yuan, Y. Fu, L. Gao, X. Ma, Comparison and theoretical analysis of the photocatalytic performance of Ni^{2+}-Fe^{3+}-CO_3^{2-}-LDHs and Ni^{2+}-Al^{3+}-CO_3^{2-}-LDHs, J. Mol. Struct., 1262 (2022) 132969, doi: 10.1016/j.molstruc.2022.132969.
[13] Y. Han, H. Li, X. Ma, Z. Liu, Preparation and formation process of Ni^{2+}–Fe^{3+} CO_3^{2-} LDHs materials with high crystallinity and well-defined hexagonal shapes, Solid State Sci., 11 (2009) 2149–2155.
[14] X. Ma, H. Li, G. Zhu, L. Kang, Z. Liu, Hydrothermal preparation and anion exchange of Co^{2+}–Ni^{2+}–Fe^{3+} CO_3^{2-} LDHs materials with well regular shape, Colloids Surf., A, 371 (2010) 71–75.
[15] P.R. Lestari, T. Takei, N. Kumada, Novel ZnTi/C_3N_4/Ag LDH heterojunction composite for efficient photocatalytic phenol degradation, J. Solid State Chem., 294 (2021) 121858, doi: 10.1016/j.jssc.2020.121858.
[16] A. Grover, I. Mohiuddin, A.K. Malik, J.S. Aulakh, K.-H. Kim, Zn-Al layered double hydroxides intercalated with surfactant: synthesis and applications for efficient removal of organic

dyes, J. Cleaner Prod., 240 (2019) 118090, doi: 10.1016/j.jclepro.2019.118090.
[17] N. El Houda Hadj-Abdelkader, B. Abdellah, Z. Ghandour, A. Nunes-Beltrao, F. Belkhadem, R. Roy, A. Azzouz, NiTiFe and NiTiZn LDHs with affinity for hydrogen – role of the surface basicity, Int. J. Hydrogen Energy, 44 (2019) 7934–7942.
[18] Y. Chen, J. Yan, D. Ouyang, L. Qian, L. Han, M. Chen, Heterogeneously catalyzed persulfate by CuMgFe layered double oxide for the degradation of phenol, Appl. Catal., A, 538 (2017) 19–26.
[19] P. Bobde, R.K. Patel, D. Panchal, A. Sharma, A.K. Sharma, R.S. Dhodapkar, S. Pal, Utilization of layered double hydroxides (LDHs) and their derivatives as photocatalysts for degradation of organic pollutants, Environ. Sci. Pollut. Res., 28 (2021) 59551–59569.
[20] X. Fan, Q. Cao, F. Meng, B. Song, Z. Bai, Y. Zhao, D. Chen, Y. Zhou, M. Song, A Fenton-like system of biochar loading Fe–Al layered double hydroxides (FeAl-LDH@BC)/H_2O_2 for phenol removal, Chemosphere, 266 (2021) 128992, doi: 10.1016/j.chemosphere.2020.128992.
[21] S. Jayaprakash, N. Dewangan, A. Jangam, S. Das, S. Kawi, LDH-derived Ni–MgO–Al_2O_3 catalysts for hydrogen-rich syngas production via steam reforming of biomass tar model: effect of catalyst synthesis methods, Int. J. Hydrogen Energy, 46 (2021) 18338–18352.
[22] K. Li, S. Li, Q. Li, H. Liu, W. Yao, Q. Wang, L. Chai, Design of a high-performance ternary LDHs containing Ni, Co and Mn for arsenate removal, J. Hazard. Mater., 427 (2021) 127865, doi: 10.1016/j.jhazmat.2021.127865.
[23] M. Falk, A.G. Miller, Infrared spectrum of carbon dioxide in aqueous solution, Vib. Spectrosc., 4 (1992) 105–108.
[24] P. Yekan Motlagh, A. Khataee, T. Sadeghi Rad, A. Hassani, S.W. Joo, Fabrication of ZnFe-layered double hydroxides with graphene oxide for efficient visible light photocatalytic performance, J. Taiwan Inst. Chem. Eng., 101 (2019) 186–203.
[25] V. Melchor-Lagar, E. Ramos-Ramírez, A.-A. Morales-Pérez, I. Rangel-Vázquez, G. Del Angel, Photocatalytic removal of 4-chlorophenol present in water using ZrO_2/LDH under UV light source, J. Photochem. Photobiol., A, 389 (2020) 112251, doi: 10.1016/j.jphotochem.2019.112251.
[26] S. Qiu, D. Zhao, Y. Feng, M. Li, X. Liang, L. Zhang, Y. Luo, K. Zhang, F. Wang, Adsorption performance and mechanism of Ca–Al-LDHs prepared by oyster shell and pop can for phosphate from aqueous solutions, J. Environ. Manage., 303 (2022) 114235, doi: 10.1016/j.jenvman.2021.114235.
[27] J.-H. Shen, Z.-W. Jiang, D.-Q. Liao, J.-J. Horng, Enhanced synergistic photocatalytic activity of TiO_2/oxidant for azo dye degradation under simulated solar irradiation: a determination of product formation regularity by quantifying hydroxyl radical-reacted efficiency, J. Water Process Eng., 40 (2021) 101893, doi: 10.1016/j.jwpe.2020.101893.
[28] G. Mikami, F. Grosu, S. Kawamura, Y. Yoshida, G. Carja, Y. Izumi, Harnessing self-supported Au nanoparticles on layered double hydroxides comprising Zn and Al for enhanced phenol decomposition under solar light, Appl. Catal., B, 199 (2016) 260–271.
[29] B.S. Marques, K. Dalmagro, K.S. Moreira, M.L.S. Oliveira, S.L. Jahn, T.A. de Lima Burgo, G.L. Dotto, Ca–Al, Ni–Al and Zn–Al LDH powders as efficient materials to treat synthetic effluents containing o-nitrophenol, J. Alloys Compd., 838 (2020) 155628, doi: 10.1016/j.jallcom.2020.155628.
[30] A. Mantilla, F. Tzompantzi, J.L. Fernández, J.A.I.D. Góngora, R. Gómez, Photodegradation of phenol and cresol in aqueous medium by using Zn/Al+Fe mixed oxides obtained from layered double hydroxides materials, Catal. Today, 150 (2010) 353–357.
[31] Y. Li, H. Bi, Y. Jin, Facile preparation of rhamnolipid-layered double hydroxide nanocomposite for simultaneous adsorption of p-cresol and copper ions from water, Chem. Eng. J., 308 (2017) 78–88.
[32] A. Mantilla, F. Tzompantzi, J.L. Fernández, J.A.I.D. Góngora, R. Gómez, Photodegradation of phenol and cresol in aqueous medium by using Zn/Al+Fe mixed oxides obtained from layered double hydroxides materials, Catal. Today, 150 (2010) 353–357.
[33] C. Tai, X. Gu, H. Zou, Q. Guo, A new simple and sensitive fluorometric method for the determination of hydroxyl radical and its application, Talanta, 58 (2002) 661–667.

Supporting information

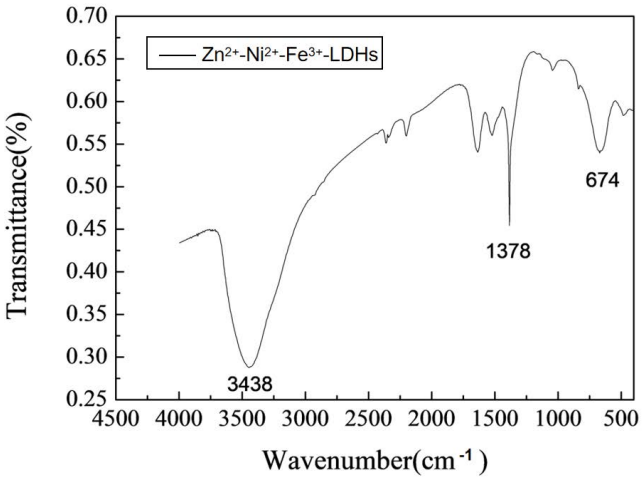

Fig. S1. FTIR spectrum of samples.

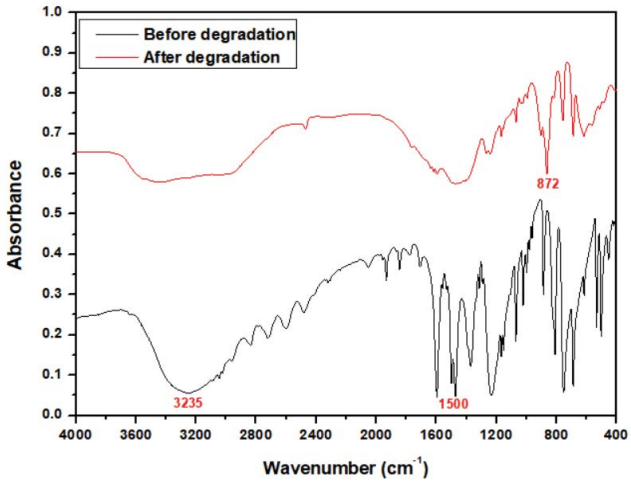

Fig. S2. FTIR spectrum of phenol solution before and after degradation.

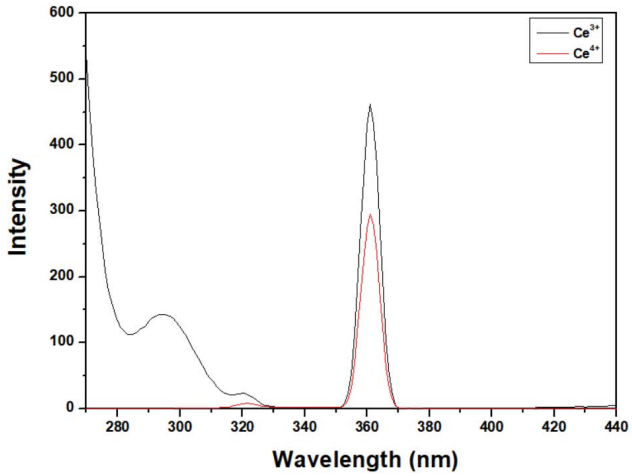

Fig. S3. Determination of hydroxyl radicals.